

Magnetic and resistivity imaging of a probable fault within the Precambrian crystalline rocks in Ogbomoso, Southwestern Nigeria

Oyelowo Gabriel BAYOWA^{1,*} , Olamide FAWOLE¹,
Martins Olusola OLORUNFEMI² , Sordiq Obafemi AJAGBE¹,
Ademakinwa George ONI² , Isaiah Oluwadara ADELERE¹,
Monsur Olawale AJIBADE¹, Febisola Esther AJIBOLA¹

¹ Department of Earth Sciences, Ladoko Akintola University of Technology,
P.M.B. 4000, Ogbomoso, Nigeria

² Department of Geology, Obafemi Awolowo University, Ile-Ife, Nigeria

Abstract: A linear structure which is interpreted to be a fault was identified within the Precambrian basement complex rocks of the Ogbomoso Southwest Sheet 222 geological map, southwest Nigeria. The ground magnetic and electrical resistivity methods were used to investigate the structure and determine its physical characteristics. Five (5) traverses with lengths varying from 700–800 m and trending approximately NW–SE were established perpendicularly to the suspected fault. Total magnetic field data were acquired at 10 m interval, corrected for diurnal variation and inverted into 2D magnetic models using the *Geosoft Oasis montaj* software package. Dipole-Dipole resistivity data were acquired along the traverses using a dipole length of 20 m with expansion factor n varying from 1 to 5 and modelled to generate 2D resistivity structures with the DIPPROTM software package. Thirty-seven (37) depth sounding datasets were acquired, quantitatively interpreted and the results used to generate geoelectric sections across the suspected geologic feature. Three major magnetic dyke lineaments D_1 , D_2 and D_3 (60–164 m wide and 70– ∞ depth extent) characterised by peak negative (–44 to –81 nT) magnetic anomalies and equivalent resistivity lineaments R_1 , R_2 and R_3 (50–140 m wide and 40 to >60 m depth extent) typified by low resistivity (10–750 Ω m) vertical discontinuities were delineated. The northern edges of lineaments D_2 and R_2 coincide significantly with the spatial location of the suspected fault F^1 – F^1 while D_1 and R_1 and D_3 and R_3 correlated and are newly identified parallel faults F^2 – F^2 and F^3 – F^3 to F^1 – F^1 and probably syngenetic with it. Geological observation of laterally displaced segments of porphyroclastic gneiss and absence of significant vertical displacement of the basement bedrock shoulders (from 2D magnetic and resistivity images and geoelectric sections) suggest that F^1 – F^1 is a strike slip fault.

*corresponding author, e-mail: obayowa@lautech.edu.ng, phone: +234803 82 0291

Key words: ground magnetic, electrical resistivity, Precambrian basement complex, strike slip fault, Southwest Nigeria

1. Introduction

In a typical crystalline rock underlain terrain, fault is a weak zone with low effective stress/strength within the competent/fresh host bedrock. This low effective strength usually results in physical properties (density, magnetic susceptibility, electrical resistivity/conductivity etc.) perturbation in the fault zone and thereby makes it manifest as a measurable physical property contrast with the host fresh bedrock. Fault may be shallow or deep. A shallow fault (with relatively thin overburden cover) may be hazardous to the environment as it may be associated with ground subsidence and act as conduit for water seepages within an area if too close to the surface (*Ojo and Olorunfemi, 1995; Ehuwole and Olorunfemi, 2012; Akinlabi and Bayowa, 2021*), or lead to failure of foundation of civil engineering structures (e.g. *Sangodiji and Olorunfemi, 2013*). Whereas a deep fault zone (with significantly thick overburden cover) could be advantageous in that it could host groundwater (*Okunubi and Olorunfemi, 2016; Olorunfemi et al., 2020*) and mineral resources (*Blain, 2000; Nabighian and Astem, 2002; Akinlalu et al., 2016; Horo et al., 2020 and Liba et al., 2022*). Such faults can also act as reservoir for geothermal energy in areas where the subsurface basement rocks have been tectonically distressed insitu (*Kana et al., 2015*). Hence, in view of the numerous importance of faults, it is usually very important that adequate information is gathered on such geologic structure for future sustainable development in an area.

Ogbomoso Sheet 222 geological map, compiled by the Geological Survey of Nigeria (*GSN, 1973*), shows an inferred and approximately ENE–WSW trending major linear geological structure suspected to be a fault that cuts across a displaced segments of a porphyroclastic gneiss (Fig. 1). The referenced fault falls within the developing settlements of Olukunle, Orile-Oje and Awode in Ogbomoso metropolis, southwestern Nigeria (Fig. 1). The fault is a geological inference that is yet to be corroborated by direct (mechanical drilling) or indirect (remote sensing, airborne or ground geophysical) investigation(s) to the knowledge of the authors. It becomes imperative therefore, that the existence of the structural feature be established

and accurately located considering the prospects and hazards of faults outlined above.

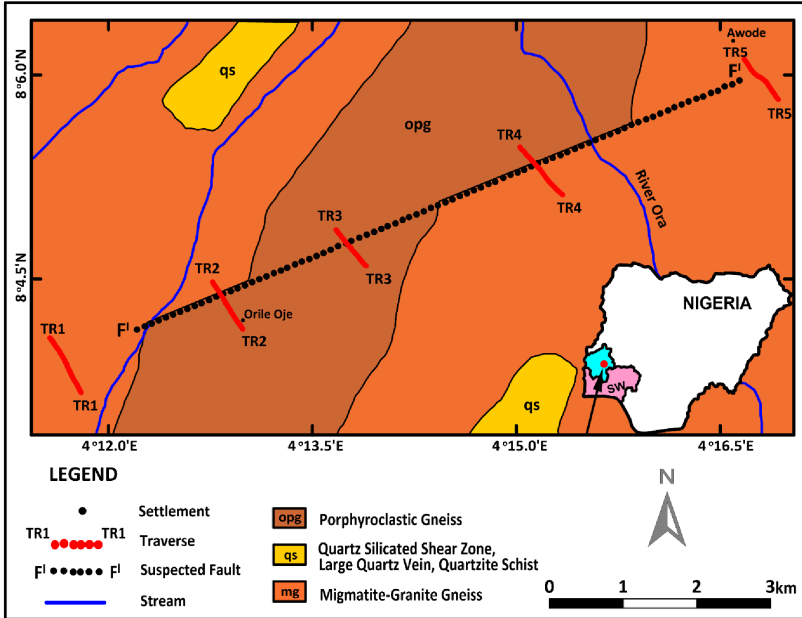


Fig. 1. Geological map of the study area (modified after *GSN, 1973*) showing the suspected fault F¹ – F¹ (inset is the map of Nigeria showing the location of the study area).

The physical property contrast (in resistivity, magnetic susceptibility, density etc.) between the fault zone and the host fresh bedrock makes the former amenable to geophysical mapping. *Oladunjoye et al. (2016)* investigated suspected Banded Iron Formation (BIF) in Ajase and Gbede areas of Ogbomosho, southwestern Nigeria (latitudes 08°00' and 08°30' N and longitudes 04°00' and 04°30' E) for its style of occurrence and the related structures using the aeromagnetic data. It characterised the acclaimed structurally controlled BIF as typified by positive residual magnetic anomalies while the total horizontal derivative derived brittle lineaments were associated with fractures and faults. The delineated lineaments mostly trend NE–SW and NW–SE with few ones trending E–W. The current study area occupies a very small portion at the central southern part of the area covered by the referenced publication. However, this publication did not clearly identify the ENE–WSW trending geologically inferred strike slip fault cur-

rently being investigated. *Ahmed et al. (2018)* also analysed the aeromagnetic data that covered both the sedimentary and basement complex regions of the southwestern Nigeria (latitudes 06°00' and 08°00' N and longitudes 02°40' and 05°00' E) and established lineaments that trend majorly NE–SW, NW–SE and NNE–SSW. It linked the NE–SW lineaments with structures emanating from the Atlantic Ocean and the NNE–SSW with the Ifewara – Kalangai fault axis. The results obtained from the very large area covered by the authors are too regional to be of relevance to the sandwiched very tiny current study area.

However, geophysical investigation is often required for the confirmation of the geological structures inferred from routine geological mapping whose locations are often subjected to spatial error while the geometry and characteristics usually require further investigation. The present study investigated the characteristics (lateral extent, width, depth extent and orientation) of the suspected structural feature in order to provide information for government and other stake holders interested in future groundwater and/or engineering infrastructural development within the study area (e.g., *Olorunfemi et al., 2000; Sangodiji and Olorunfemi, 2013; Fatoba et al., 2015 and Fatoba et al., 2018*). The outcome of the study can also be an update information on the existing structures within the Ogbomoso Sheet 222 geological map.

Geophysical survey involving ground magnetic and electrical resistivity (Electrical Resistivity Tomography (ERT) and Vertical Electrical Sounding (VES)) methods was deployed in the study to image the suspected fault. The magnetic and electrical resistivity geophysical methods have found useful applications in the mapping of geological structures such as rock contacts, fractures/faults and shear zones within the hard rock terrains (e.g., *Brownfield and Charpentier, 2006; Ramesh Babu et al., 2007; Ishola et al., 2010; Kayode and Adelusì, 2010; Bayode and Akpoarebe, 2011; Kaki et al., 2013; Sangodiji and Olorunfemi, 2013; Omenda, 2018; Olorunfemi and Oni, 2019; Olorunfemi et al., 2020; Olorunfemi et al., 2021 and Liba et al., 2022*). This implies that significant magnetic susceptibility and electrical resistivity contrasts are expected to exist between such geological features and the host crystalline rocks (e.g. *Olorunfemi et al., 1986; Valtr and Hanžl, 2008; Sangodiji and Olorunfemi, 2013; Olorunfemi et al., 2020; Akinlabi and Bayowa, 2021*). Both the ground magnetic and electrical resis-

tivity geophysical methods are cheap, and non-invasive in comparison with direct and invasive investigation technique such as mechanical drilling.

The objectives of the study are to locate the position of the suspected fault accurately on the ground, gather, process and interpret ground magnetic and electrical resistivity data along established traverses across the suspected geologic feature and draw appropriate inference on the geometry and characteristics of the linear structure.

1.1. Study area description and geological setting

The study area is located within the southern part of Ogbomoso, Southwestern Nigeria. It lies between latitudes $08^{\circ}03.4'$ and $08^{\circ}06.6'$ N and longitudes $04^{\circ}11.6'$ and $04^{\circ}17.2'$ E (Fig. 1) and falls within the tropical climatic region that is characterized by high temperatures, relatively high humidity, and two rainfall regimes. The mean temperature averages 28°C between mid January and March (*Abuloye et al., 2017*). The vegetation is the rain forest type composed of tall trees mixed with thick undergrowth. The area is drained by Rivers Adunyin, Ora, Oba and Odoje and the drainage pattern is dendritic (Fig. 1).

Ogbomoso area is underlain by the Basement Complex Rocks (*Rahaman, 1971, 1973; Obaje, 2009; Oluyide et al., 1998* and *Akinloye et al., 2002*) (Fig. 1). The basement rocks belong to the Migmatite-Gneiss-Quartzite Complex group. Four rock types characterize the study area. The rock types include granite gneiss, the undifferentiated migmatite gneiss, the porphyroclastic gneiss and the centrally emplaced quartzites (*Rahaman, 1976; Oluyide et al., 1998* and *Afolabi et al., 2013*) (Fig. 1). The major geological structures in the area include strike slip faults mapped from geological field observations and curve-linear structures (lineaments) delineated from satellite images (*Afolabi et al., 2013*).

2. Materials and methods

Topographical, geological and administrative maps, relevant to this study, were obtained from various archives. The maps were digitized to ensure accuracy of positions. The bounding coordinates of the suspected feature were extracted from Ogbomoso Southwest Sheet 222 geological map. The Global

Positioning System (GPS) was used to position the probable structural feature on the ground during fieldwork using the estimated coordinates from the geological map.

For maximum target resolution, five (5) traverses designated by TR1 (700 m), TR2 (700 m), TR3 (700 m), TR4 (800 m), and TR5 (700 m) (Figs. 1, 2), were established approximately normal to the approximately ENE–WSW trending suspected fault ($F^1 - F^1$). The traverse-traverse separation varied from 2.0–4.0 km. The length of the suspected structural feature was estimated from the geologic map to be about 8 km. The geographical co-ordinates of all the stations along each traverse were determined with the GPS.

The ground magnetic and the electrical resistivity (ERT and VES) methods were employed. The magnetic method was deployed as a quick reconnaissance technique for the identification of basement structures (*Olorunfemi et al., 2020*). Magnetic profilings were carried out along the five (5) traverses using the GSM-19T Proton Precession Magnetometer. The total magnetic field measurements were taken at 10 m interval. With a sensor height at 1.5 m, two measurements were made per station and the time of measurement recorded. Diurnal variation correction was applied (*Sharma, 1987*) and three points running mean filter was carried out on the corrected magnetic data to remove noise arising from cultural effects. The reduced magnetic data were used to generate magnetic profiles. The data interpretation was both qualitative and quantitative (*Okunubi and Olorunfemi, 2016; Olorunfemi and Oni, 2019* and *Olorunfemi et al., 2020*). The magnetic profiles were quantitatively interpreted by block modelling using the Oasis Montaj version 6.4.2 software with local geomagnetic elements of inclination (I) = -10.3° , declination (D) = -1.2° and the total field magnetic intensity (F) = 32, 809 nT. Estimation of the anomaly characteristics is more reliable with modelling of the magnetic profiles which position and bring the anomalous zones to their true positions in the subsurface. Hence, model sections are obtained. Detailed description of the quantitative interpretation of the magnetic profiles is contained in *Olorunfemi et al. (2020)*.

2D subsurface resistivity imaging, using the ERT and adopting the dipole-dipole array was carried out along the five traverses TR1-5 whose lengths vary from 700–800 m. The choice of dipole-dipole array in this study is based on its good depth of penetration although its vertical resolution could

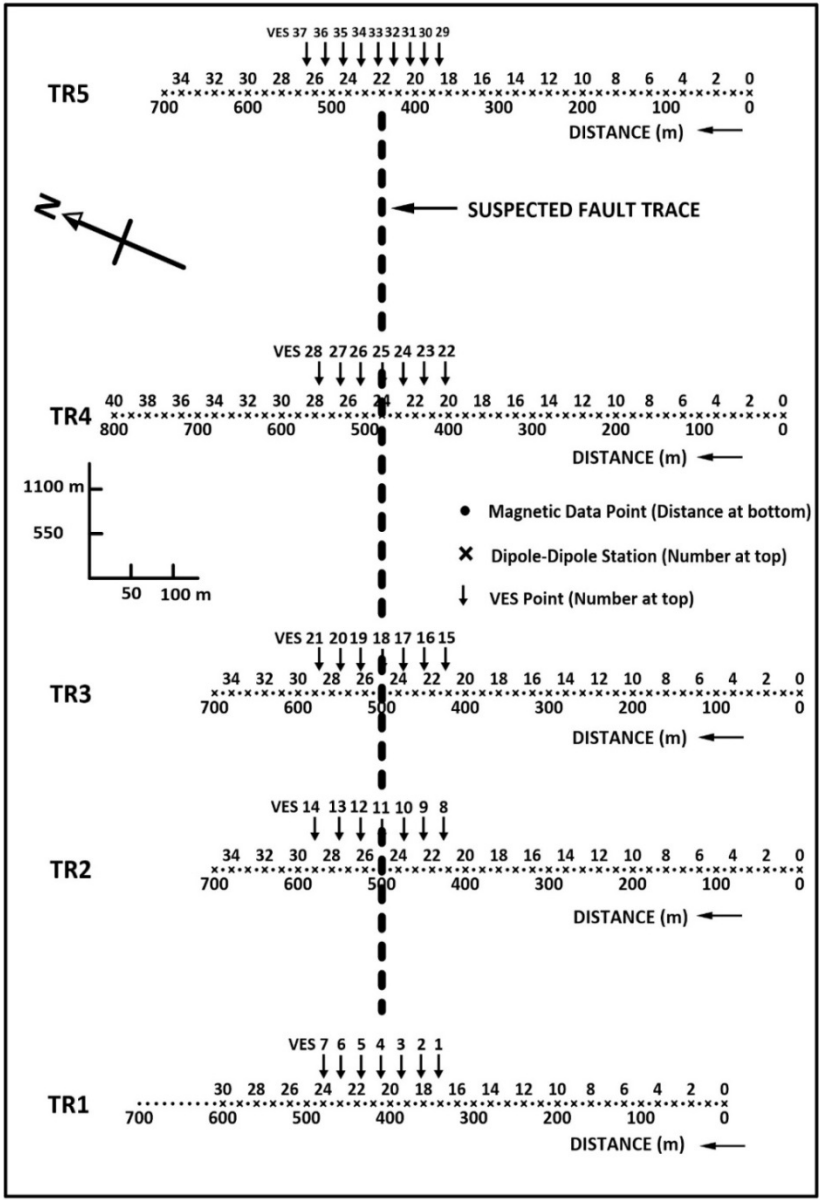


Fig. 2. Field layout and geophysical data acquisition map showing the established traverses, magnetic data points, dipole-dipole stations and VES data points.

be poor at deep depth (*Reynolds, 2011*). Measurements were made with a dipole length of 20 m and an expansion factor (the distance between the leading potential electrodes and the trailing current electrodes), n , ranging from 1 to 5. DIPPRO™ software package (*Dippro, 2004*) was used to invert the resulting apparent resistivity data in order to obtain 2D resistivity structures (migrated images) of the subsurface beneath the established traverses. The computer program utilises smoothness constrained least squares method (*Sasaki, 1992*) to automatically develop a 2D resistivity structure of the subsurface from a set of field observed 2D (dipole-dipole) resistivity data (*Omowumi, 2018*). A 3-layer model evolved from the VES interpretation results (see Fig. 5), was adopted for the field environment and used to constrain the 2D inversion modelling.

Thirty-seven (37) VES stations, using the Schlumberger array were established across the suspected fault $F^1 - F^1$ zone. The VES interval was 25 m along traverses 1–4 and 20 m along traverse 5 with length of coverage of 150–200 m and the fault trace kept at the centre (Fig. 2). The current electrode spacing ($AB/2$) ranged between 1 and 100 m. The VES data acquisition was done with the ABEM SAS 1000 Resistivity Meter. The apparent resistivity data obtained were interpreted quantitatively with the partial curve matching technique (*Mooney and Wetzel, 1954*) to obtain preliminary layer parameters (resistivities and thicknesses) used as starting model parameters in WinResist version 1.0 software 1D forward modelling to obtain the true layer resistivities and thicknesses (*Bayowa et al., 2021*). The true layer parameters were used to generate 2D geoelectric images (sections) beneath the established traverses.

The ground magnetic, ERT and VES results were integrated to establish and determine the geometry and physical characteristic of the suspected fault.

3. Results and discussion

3.1. Ground magnetic imaging

Figures 3a-e present stacked observed residual total magnetic field profiles, the theoretically generated equivalents and the 2D magnetic models along correlated traverses 5–1. The residual magnetic profiles vary in amplitudes from -81 to $+68$ nT and are characterised by typical thin (peak negative

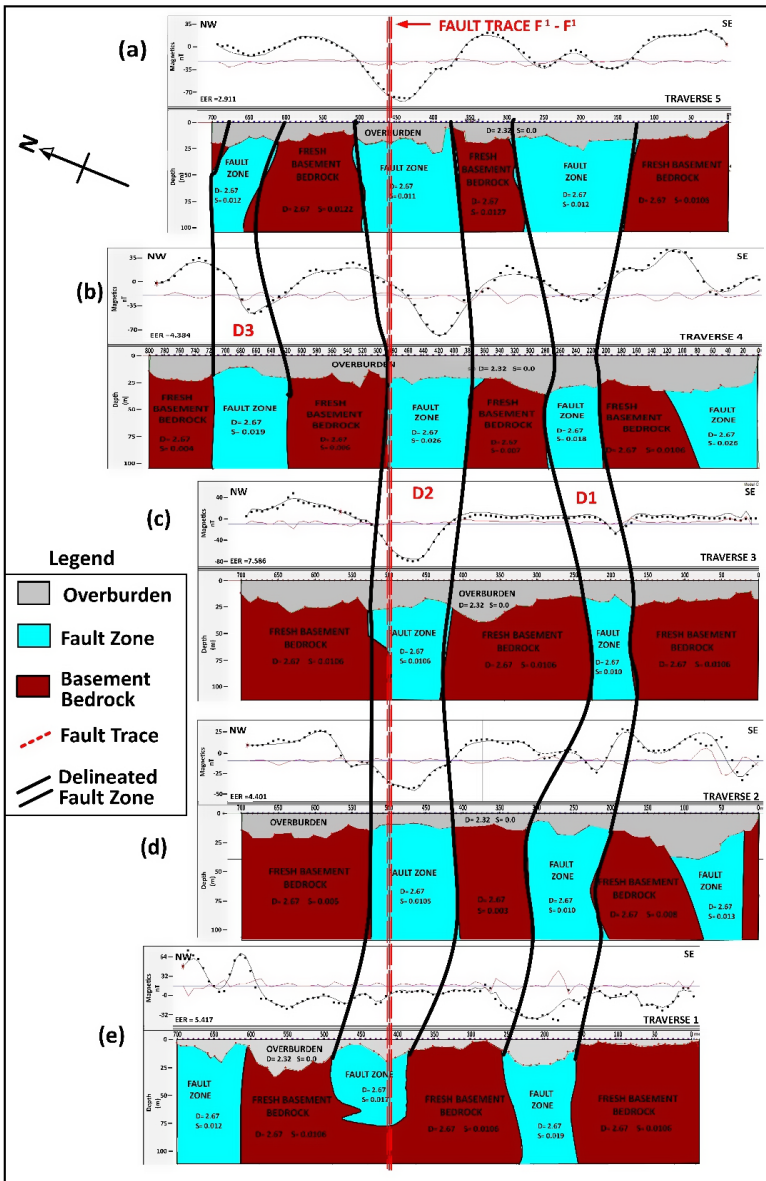


Fig. 3. Stacked magnetic profiles (black dots) and model responses (solid black curve) along (a) traverse 1 (b) traverse 2 (c) traverse 3 (d) traverse 4 and (e) traverse 5. Fault trace on the geological map is shown by solid red curve.

amplitude magnetic anomaly bothered on both sides by low-amplitude positive magnetic shoulders) and thick dyke (double-negative peak amplitude magnetic anomalies with central low-amplitude positive peak flanked on both sides by low-amplitude positive peak anomaly shoulders) anomalies (Parasnis, 1986).

The magnetic profiles were modelled into alternating blocks of fresh basement (in brownish colour) and thin/thick dikes (Sheriff, 1991 and Abdelrahman and Essa, 2005) (in light blue colour) with the dikes representing fault zones. The modelled overburden thicknesses range from a minimum of 1.5 m beneath traverse 1 to a maximum of 40 m beneath traverse 3 (Fig. 3). The spatial location and the characteristics of the modelled fault zones are contained in Table 1. The zones correlate across the traverses as approximately ENE–WSW trending lineaments D₁, D₂ and D₃ (Fig. 3). The northern edge of fault zone D₂ virtually correlate with the suspected fault trace F¹–F¹. Similar coincidence of the edge of anomalous magnetic and resistivity zone with the spatial location of a fault trace was observed by Olorunfemi et al. (2020). Traverses 2 and 3 are not long enough to establish if D₃ continues WSW even though a modelled fault zone at the northwestern edge of traverse 1 indicates a possibility.

Table 1. Characteristics of interpreted fault zones from the 2D magnetic models.

Trav. (TR)	Fault Zone 1		Fault Zone 2		Fault Zone 3		Fault Zone 4	
	Dist./Width (m)	DEx (m)	Dist./Width (m)	DEx (m)	Dist./Width (m)	DEx (m)	Dist./Width (m)	DEx (m)
5	121–285/164	∞	378–509/129	∞	600–678/78	∞	–	–
4	0–126/126	∞	210–270/60	∞	370–490/120	∞	620–714/94	∞
3	170–40/70	∞	415–520/105	∞	–	–	–	–
2	20–115/95	∞	193–300/107	∞	414–525/111	∞	–	–
1	157–257/100	75	385–478/93	∞	600–700/100	∞	–	–

Note: Trav.: Traverse; Dist.: Distance; DEx: Depth Extent. Distance 0 is at the SE end of the traverses with profiling in the direction of the NW.

While D₂ establishes the existence of the suspected fault F¹–F¹, correlated fault zones D₁ and D₃ indicate the likelihood of the existence of two parallel and syngenetic faults F²–F² and F³–F³.

3.2. ERT

Figures 4a-e depict the correlated ERT images beneath traverses 1–5. The modelled subsurface resistivity values range from 10–14,000 Ωm across the survey area. The images classify the subsurface into four subsurface geologic units which include the topsoil, weathered layer, fractured basement and fresh basement. The topsoil is thin ($< 5\text{ m}$) and subsumed into the much

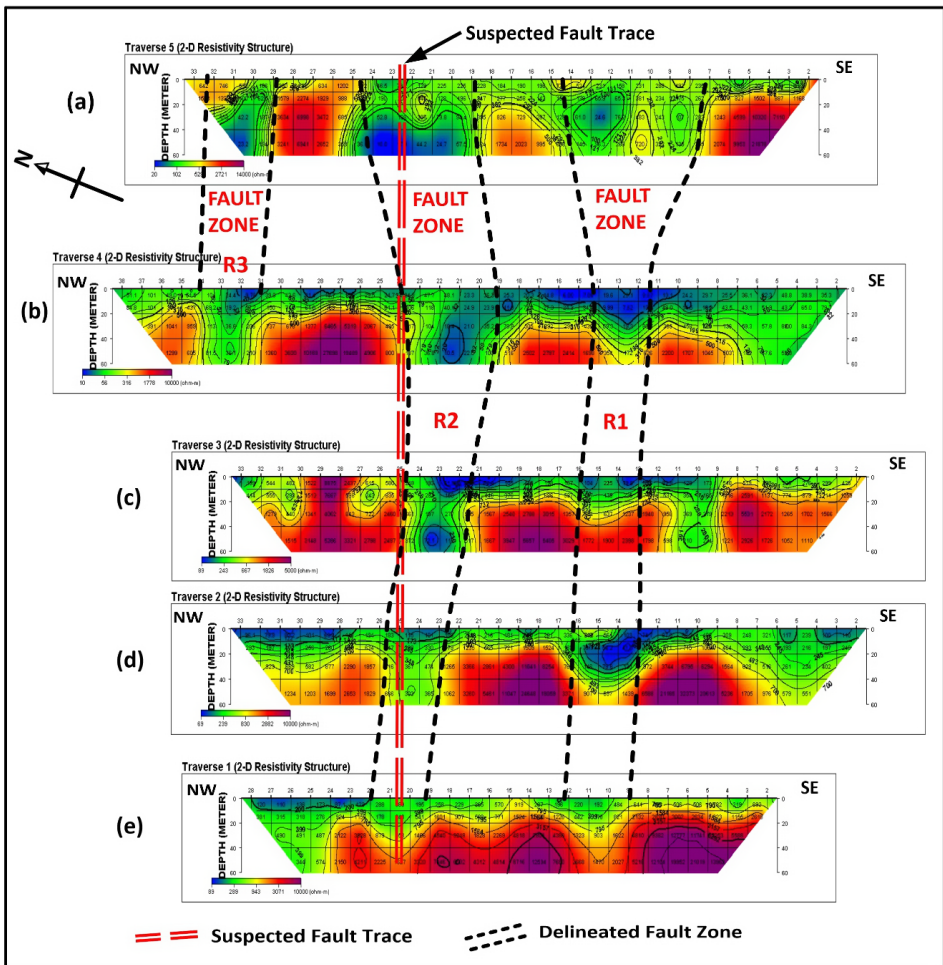


Fig. 4. Stacked 2D resistivity structures along (a) traverse 5 (b) traverse 4 (c) traverse 3 (d) traverse 2 and (e) traverse 1.

thicker weathered layer with overlapping resistivity values. The topsoil resistivity values range between 10 and >1,000 Ωm. The weathered layer has very low resistivity with values ranging between 10 and 500 Ωm and estimated thickness of 4–20 m. The fractured basement columns which manifest as vertical to near-vertical low resistivity discontinuity sandwiched between adjacent very high resistivity fresh basement (*Olorunfemi et al., 2020*) with resistivity values overlapping with that of the weathered layer where the column is deeply weathered and groundwater saturated. The resistivity values could be as high as 750 Ωm or more at the transition zone. Estimates of the depth extent range from 40 to >60 m. The fresh basement displays resistivity values that are generally >750 Ωm and could be as high as 14,000 Ωm. The overburden thicknesses generally range from about 5 m to 30 m where fractured basements were not delineated.

The suspected fractured basement zones with anomalously low resistivity were mapped at distances indicated in Table 2 along each traverse with estimated width and depth extents. The anomalous zones R₁, R₂ and R₃ correlate across the traverses (Fig. 4) to give an approximately ENE–WSW trending lineaments. The northern edge of the resistivity anomalous zone R₂ significantly coincide with the spatial trace of suspected fault F¹–F¹ (Fig. 1) which is the subject matter of this investigation. Anomalous zone R₂ also cut across all the traverses while zone R₃ could only be correlated across traverses 4 and 5 while traverses 1–3 may not have been long enough to intercept the linear feature. The linear features R₂ and R₃ are suspected to be faults F²–F² and F³–F³.

Table 2. Spatial characteristics of resistivity anomalous zones from 2D images.

Trav. (TR)	Anomalous Zone R ₁			Anomalous Zone R ₂			Anomalous Zone R ₃		
	Dist. (m)	Width (m)	Depth (m)	Dist. (m)	Width (m)	Depth (m)	Dist. (m)	Width (m)	Depth (m)
5	140–280	60	>60	380–490	110	>60	580–640	60	>60
4	230–280	50	60	380–480	100	>60	620–680	60	>60
3	260–320	60	40	420–500	80	>60	–	–	–
2	260–320	60	60	450–520	70	>60	–	–	–
1	180–240	60	40	380–440	60	50	–	–	–

Note: Trav.: Traverse; Dist.: Distance.

While the stacked 2D images has corroborated the existence of suspected fault $F^1 - F^1$, it has also established two other parallel and possibly syn-genetic suspected faults $F^2 - F^2$ and $F^3 - F^3$.

3.3. VES imaging

The VES interpretation results are displayed in Table 3 and graphically presented as correlated geoelectric sections in Figs. 5a-e. VES stations 33, 25, 18, 11 and 4 were located across the traverses to coincide with the suspected fault trace. The geoelectric sections delineate three (3) subsurface layers which are the topsoil, weathered layer and the partly weathered/fractured/fresh basement bedrock. The geoelectric characteristics beneath the traverses are contained in Table 4. For the survey area, the topsoil resistivity and thickness ranges are 43–4,356 Ωm and 0.9–2.4 m respectively while for the weathered layer; 9–662 Ωm (but generally < 150 Ωm) and 0.7–36.1 m; and the partly weathered/fractured/fresh basement in the range of 102–11,160 Ωm (but generally > 1,000 Ωm) and depth to rock head of 1.8–38.6 m (Table 4). These geoelectrical parameters correlate significantly with those derived from the 2D images and as observed by *Idornigie et al. (2006)*; *Olorunfemi (2008)* and *Olorunfemi (2020)* in similar basement complex environments.

Except along traverse 1, the fault trace falls within and at about the center of basement depressions. Fault zones are regions of weakness typified by high degree of water saturation and weathering leading to relatively thick weathering depths and basement depressions (*Olorunfemi et al., 1986*). The fault diagnostic basement depressions are wide (100–150 m) beneath traverses 5 (VES 35-30) and 4 (VES 28-22) becoming narrower (50–70 m) along traverses 3 (VES19-17) and 2 (VES 12-9) and virtually non-existent along traverse 1. These width extent correlate significantly with the geometry of the delineated anomalous zone R_2 (see Table 2) across the traverses.

3.4. Synthesis

The study area is characterised by three major magnetic dyke lineaments D_1 , D_2 and D_3 (Fig. 3) that trend approximately ENE–WSW with width extents of 60–164 m and linear extent possibly in excess of 8 km. the northern edge of lineament D_2 significantly coincide with the spatial location of

Table 3. VES interpretation results.

VES No.	DEPTH (m)	LAYER RESISTIVITIES (ohm-m)
1	1.4/7.2	2339/109/775
2	0.9/2.4	113/13/1269
3	1.0/1.8/18.4	54/15/308/6889
4	1.1/1.4/2.1/7.9	43/68/9/953/3588
5	1.0/3.5	900/37/1620
6	0.9/2.7/20.7	109/57/476/2902
7	1.1/6.8	537/95/4823
8	1.3/4.0	412/132/743
9	1.1/1.7/5.7	283/239/91/2823
10	1.1/9.4	300/104/1439
11	1.4/15.9	300/142/5798
12	1.1/5.6	256/77/676
13	1.0/9.3	448/125/2393
14	0.9/5.6/18.6	397/84/778/2502
15	1.0/15.0	396/120/2920
16	0.9/8.5	2976/72/6526
17	0.8/5.9	1517/38/995
18	1.2/8.0	1554/67/7013
19	1.2/2.4/7.4	2475/782/87/3748
20	1.8/12.0	1902/309/4121
21	1.7/16.1	4356/562/11160
22	1.6/16.8	96/18/152
23	1.2/30.3	94/22/619
24	1.0/1.9/34.3	262/55/38/529
25	1.0/4.0/27.4	143/39/18/359
26	1.1/2.1/29.2	357/178/35/223
27	0.9/2.8/27.5	64/118/29/1664
28	1.8/3.4/19.2	473/255/40/102
29	1.2/1.4/23.9	2806/3112/259/4546
30	1.2/1.9/8.4	3018/1636/161/465
31	1.3/2.1/2.5/17.6	1805/1630/487/109/942
32	1.1/1.7/13.7	2420/1793/116/1088
33	1.8/14.3	1278/81/1699
34	0.6/1.7/15.4	908/2658/88/4197
35	0.6/1.3/5.2	1510/3610/57/1770
36	1.0/4.6/28.0	3138/662/225/1647
37	1.2/1.8/38.6	2789/2398/523/4067

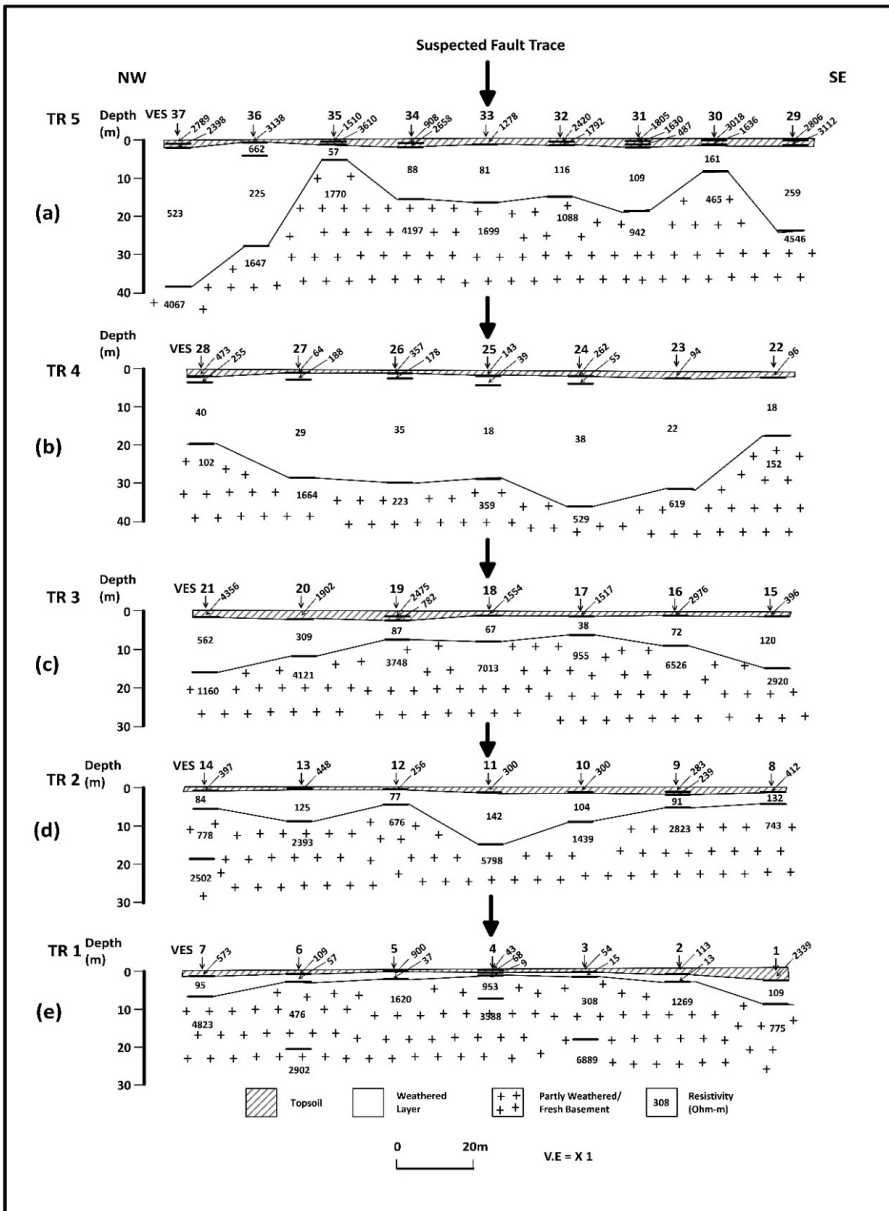


Fig. 5. Geoelectric sections along (a) traverse TR1, (b) traverse TR2, (c) traverse TR3, (d) traverse TR4, and (e) traverse TR5.

Table 4. Interpreted geoelectric characteristics beneath traverses 5 – 1.

Traverse (TR)	Lithological Description	Resistivity Range (ohm-m)	Thickness Range (m)
5	Topsoil	908 – 3,610	1.0 – 2.1
	Weathered Layer	57 – 662	3.9 – 36.1
	Partly weathered/ Fractured/Fresh Basement	465 – 4,197	5.2 – 38.6*
4	Topsoil	64 – 473	0.9 – 1.8
	Weathered Layer	18 – 255	15.2 – 33.3
	Partly weathered/ Fractured/Fresh Basement	102 – 1,664	16.8 – 34.3*
3	Topsoil	396 – 4,356	0.9 – 2.4
	Weathered Layer	38 – 562	5.1 – 14.4
	Partly weathered/ Fractured/Fresh Basement	955 – 11,160	5.9 – 16.1*
2	Topsoil	239 – 448	0.9 – 1.4
	Weathered Layer	77 – 142	2.7 – 14.5
	Partly weathered/ Fractured/Fresh Basement	670 – 5,798	4.0 – 15.9*
1	Topsoil	43 – 2,339	0.9 – 1.4
	Weathered Layer	9 – 109	0.7 – 5.7
	Partly weathered/ Fractured/Fresh Basement	308 – 4,823	1.8 – 6.8*
<hr/>			
Survey Area	Topsoil	43 – 4,356	0.9 – 2.4
	Weathered Layer	9 – 662	0.7 – 36.1
	Partly weathered/ Fractured/Fresh Basement	102 – 11,160	1.8 – 38.6*

Note: * – Depth to Rock Head

the suspected fault $F^1 - F^1$ while D_1 and D_3 are newly established faults $F^2 - F^2$ and $F^3 - F^3$.

The stacked 2D resistivity images also identify three resistivity lineaments R_1 , R_2 and R_3 (Fig. 4) that align in the same direction as the magnetic lineaments D_1 , D_2 and D_3 with width extents of 50–140 m and similarly spatially located (Fig. 6). The northern edge of resistivity lineament R_2 almost perfectly coincides with fault trace $F^1 - F^1$ while R_2 and R_3 with the newly identified faults $F^2 - F^2$ and $F^3 - F^3$. The 2D geoelectric section created across fault trace $F^1 - F^1$ display basement bedrock depressions within the fault zone.

The significant correlation between the magnetic and resistivity results and the geological field observation established the suspected fault $F^1 - F^1$ as a strike slip fault and $F^2 - F^2$ and $F^3 - F^3$ as two parallel and possibly syngenetic faults to fault $F^1 - F^1$. The three faults are spatially located on the geological map (Fig. 7).

4. Conclusions

In this study, the ground magnetic and the electrical resistivity methods have been used to investigate a suspected fault zone identified on Ogbomoso Sheet 222 published by the *GSN (1973)*. Characteristic magnetic anomalies of thin and thick dykes and low resistivity vertical discontinuities were used to map the referenced fault and other linear structures in the area. Magnetic lineaments D_1 , D_2 and D_3 and the equivalent resistivity lineaments R_1 , R_2 and R_3 were delineated across the established traverses. The northern edge of D_2/R_2 significantly coincide with the geologically established fault trace $F^1 - F^1$ while D_1/R_1 and D_3/R_3 are newly delineated faults $F^2 - F^2$ and $F^3 - F^3$ which are parallel and possibly syngenetic to fault $F^1 - F^1$.

Based on field observation (laterally displaced segments of a porphyroclastic gneiss) and insignificant relative vertical displacement of the basement bedrock across the fault zones from magnetic and resistivity 2D models, faults $F^1 - F^1$ is typically a strike slip fault. Fault zones are host for mineral deposit and groundwater storage and hence have potentials for mineral and groundwater developments for governments, individuals and the private sector. However, such zones could be inimical for building structures most especially civil engineering foundations. The results of this study have

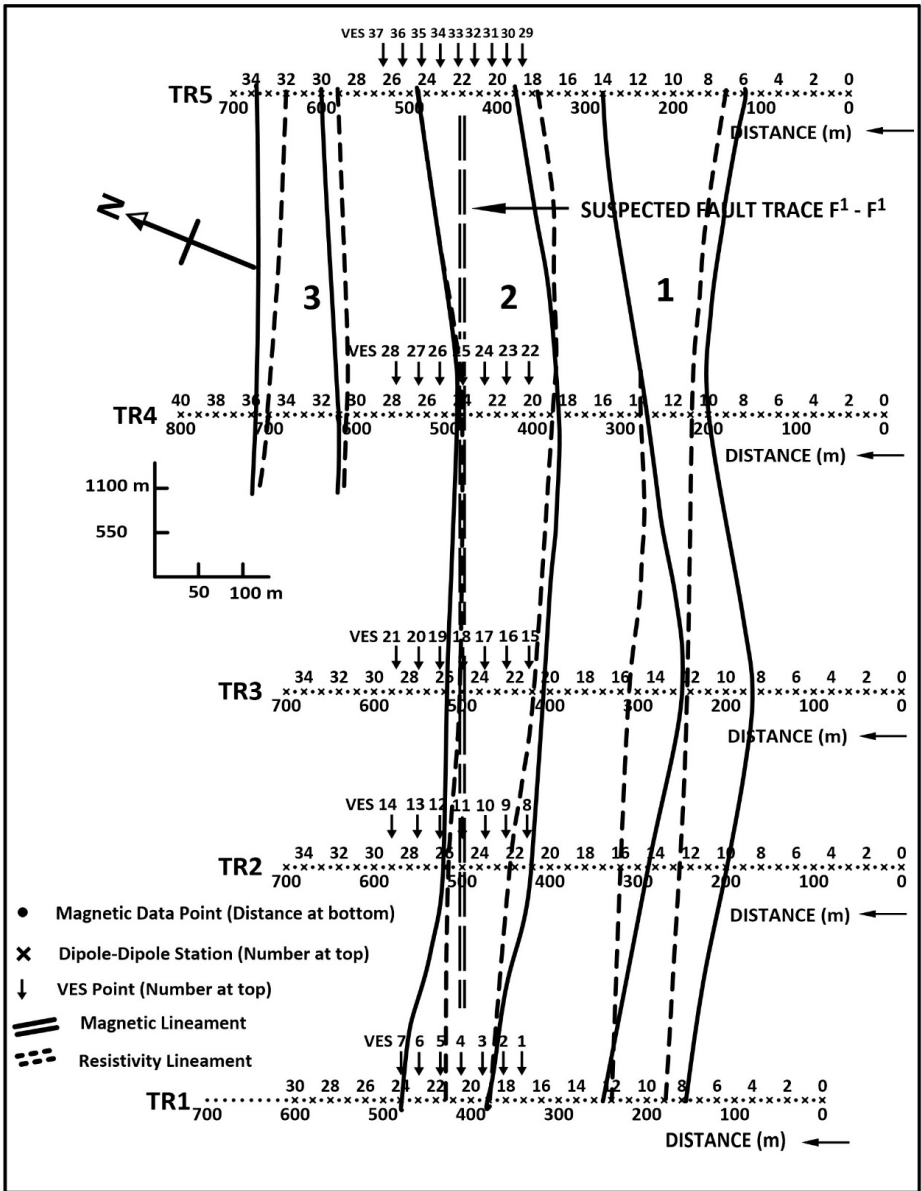


Fig. 6. Superimposed shells of magnetic (D) and resistivity (R) lineaments on the data acquisition base map.

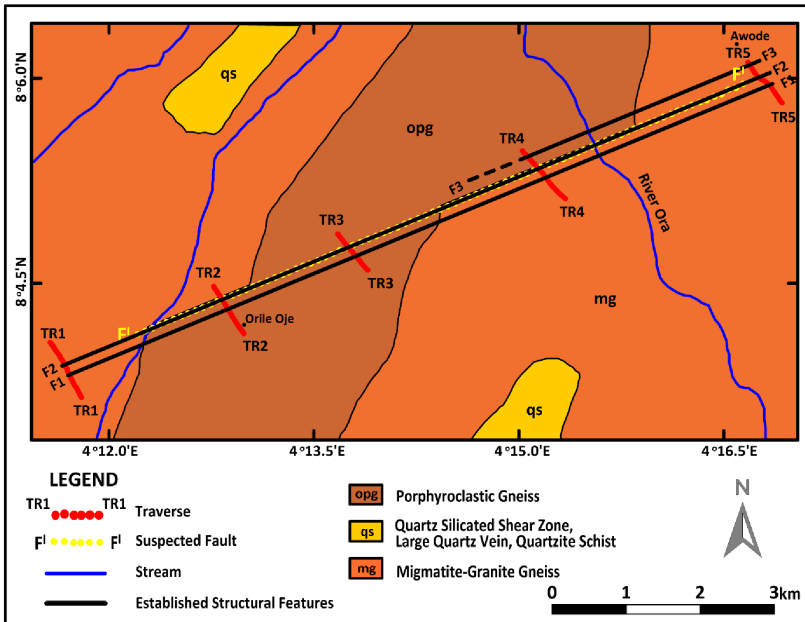


Fig. 7. Geological map showing the delineated geological structures in the study area.

also enhanced the knowledge on the structural setting of part of Ogbomosho Southwest Sheet 222.

Funding. This work does not received financial support in form of funds or grants during the preparations of the manuscript.

Competing interest. Authors have no relevant financial or non-financial interest to disclose.

Author contributions. Oyelowo Gabriel Bayowa designed and supervised the study. Oyelowo Gabriel Bayowa, Martins Olusola Olorunfemi and Isaiah Oluwadara Adelere formulated suitable methods used for the study. Oyelowo Gabriel Bayowa, Olamide Fawole, Isaiah Oluwadara Adelere, Sordiq Obafemi Ajagbe, Ademakinwa George Oni, Febisola Esther Ajibola and Monsur Olawale Ajibade anchored the data acquisition. Oyelowo Gabriel Bayowa and Martins Olusola Olorunfemi handled the literature review. Isaiah Oluwadara Adelere and Ademakinwa George Oni analysed and interpreted the data, and produced Figures 1–6. Oyelowo Gabriel Bayowa and Martins Olusola Olorunfemi prepared the final manuscript draft. All authors read manuscript and approved the final draft of the manuscript for submission.

References

- Abdelrahman E.-S. M., Essa K. S., 2005: Magnetic interpretation using a least-squares depth shape curves method. *Geophysics*, **70**, 3, L23–L30, doi: 10.1190/1.1926575.
- Abuloye A. P., Nevo A. O., Eludoyin O. M., Popoola K. S., Awotoye O. O., 2017: An Assessment of Effective Temperature, Relative Strain Index and Dew Point Temperature over Southwest Nigeria. *J. Climatol. Weather Forecast.*, **5**, 1, 192, doi: 10.4172/2332-2594.1000192.
- Afolabi O. A., Kolawole L. L., Abimbola A. F., Olatunji A. S., Ajibade O. M., 2013: Preliminary Study of the Geology and Structural Trends of Lower Proterozoic Basement Rocks in Ogbomoso, SW Nigeria. *J. Environ. Earth Sci.*, **3**, 8, 82–95.
- Ahmed Z., Lawal K. M., Ahmed A. L., 2018: Interpretation of High Resolution Aeromagnetic Data of Part of Southwestern Nigeria for Subsurface Mapping. *Dutse J. Pure Appl. Sci. (DUJOPAS)*, **4**, 2, 221–235.
- Akinlabi I. A., Bayowa O. G., 2021: 2D Electrical Resistivity Imaging of Bedrock Fissures in Ogbomoso, Southwestern Nigeria. *LAUTECH Journal of Civil and Environmental Studies*, **7**, 2, 46–54, doi: 10.36108/laujoces/1202.70.0250.
- Akinlalu A. A., Adelusi A. O., Mamukuyomi E. A., Akeredolu B. E., 2016: Ground magnetic and 2-D resistivity mapping of basement structures around Iwaraja area southwestern Nigeria. *J. Basic Appl. Res. Int.*, **18**, 4, 206–221.
- Akinloye M. K., Fadipe D. O., Adabanija M. A., 2002: A Radiometric Mapping of the Ladoke Akintola University of Technology Campus, Ogbomoso, Southwestern Nigeria. *Sci. Focus*, **1**, 55–61.
- Bayode S., Akpoarebe O., 2011: An integrated geophysical investigation of a Spring in Ibuji Igbara-Oke, southwestern Nigeria. *Ife J. Sci.*, **13**, 1, 63–74.
- Bayowa O. G., Afolabi O. A., Akinluyi F. O., Oshanaiye A. O., Adelere I. O., Mudashir A. W., 2021: Integrated geoelectric and hydrochemistry investigation for potential groundwater contamination around a reclaimed dump site in Taraa, Ogbomoso, Southwestern Nigeria. *Int. J. Energy Water Resour.*, **7**, 133–154, doi: 10.1007/s42108-021-00167-9.
- Blain C., 2000: Fifty year trends in minerals discovery – commodity and ore types. *Explor. Min. Geol.*, **9**, 1, 1–11, doi: 10.2113/0090001.
- Brownfield M. E., Charpentier R. R., 2006: Geology and total petroleum systems of the Gulf of Guinea Province of West Africa. *U.S. Geol. Surv. Bull.* 2207-C, 32 p.
- Dippro, 2004: DIPPRO™ Version 4.0: Processing and interpretation software for dipole dipole electrical resistivity data. KIGAM, Daejon, South Korea.
- Eluwole A. B., Olorunfemi M. O., 2012: Time-Lapsed geophysical investigation of the Mokuro Earth Dam Embankment, Southwestern Nigeria, for anomalous seepages. *Pacific J. Sci. Technol., USA*, **13**, 1, 604–614.
- Fatoba J. O., Eluwole A. B., Ademilua O. L., Sanuade O. A., 2018: Evaluation of subsurface conditions by geophysical methods at Ureje Earth Dam Embankment, Ado-Ekiti, Southwestern Nigeria – A case study. *Indian J. Geosci.*, **72**, 4, 275–282.
- Fatoba J. O., Olorunfemi M. O., Eluwole A. B., 2015: Subsurface structures and the effect on flexible pavement performance: The Shagamu-Benin Expressway, southwestern

- Nigeria, as case study. *Indian J. Geosci.*, **69**, 2, 137–144.
- Geology Survey of Nigeria (GSN), 1973: Geological map of Ogbomoso Sheet 222. Geological Survey of Nigeria Publication.
- Geosoft Oasis montaj, Oasis montaj How-to-Guide. Magnetic Lineament Extraction, 3D Euler Deconvolution, Magnetic Vector Inversion, <http://geosoft.com/>.
- Horo D., Pal S. K., Singh S., Srivastava S., 2020: Combined self potential, electrical resistivity tomography and induced polarisation for mapping of gold prospective zones over a part of BabaiKundi-Birgaon Axis, North Singhbhum Mobile Belt, India. *Explor. Geophys.*, **51**, 5, 507–522, doi: 10.1080/08123985.2020.1722026.
- Idornigie A. I., Olorunfemi M. O., Omitogun A. A., 2006: Electrical resistivity determination of subsurface layers, subsoil competence and soil corrosivity at an engineering site location in Akungba-Akoko, southwestern Nigeria. *Ife J. Sci.*, **8**, 2, 159–177, doi: 10.4314/ij.s.v8i2.32216.
- Ishola K. S., Adeoti L., Obianeri A., 2010: Interpretation of the historic site, Agorin in Badagry, Southwestern Nigeria using geophysical methods. *Ozean J. Appl. Sci.*, **5**, 1, 85–99.
- Kaki C., d'Almeida G. A. F., Yalo N., Amelina S., 2013: Geology and petroleum systems of the offshore Benin Basin (Benin). *Oil Gas Sci. Technol.*, **68**, 2, 363–381, doi: 10.2516/ogst/2012038.
- Kana J. D., Djongyang N., Raïdandi D., Nouck P. N., Dadjé A., 2015: A review of geophysical methods for geothermal exploration. *Renew. Sustain. Energy Rev.*, **44**, 87–95, doi: 10.1016/j.rser.2014.12.026.
- Kayode J. S., Adelusi A. O., 2010: Ground Magnetic Data Interpretation of Ijebu-Jesa Area, Southwestern Nigeria, using Total Component. *Res. J. Appl. Sci. Eng. Technol.*, **2**, 8, 703–709.
- Liba A. M., Bonde D. S., Abbas M., Usman A., Boyi D., 2022: Geophysical assessment of geologic structures associated with gold mineralisation along Garin Hausawa (Izga) using aeromagnetic data. *Int. J. Adv. Eng. Manag. (IJAEM)*, **4**, 2, 84–90, ISSN: 2395-5252, doi: 10.35629/5252-04028490.
- Mooney H. M., Wetzell W., 1954: Master curves for a two, three and four layer Earth. Univ. of Minnesota Press, Minneapolis, MM, 145 p.
- Nabighian M. N., Asten M. W., 2002: Metalliferous mining geophysics—state of the art in the last decade of the 20th century and the beginning of the new millennium. *Geophysics*, **67**, 3, 964–978, doi: 10.1190/1.1484538.
- Obaje N. G., 2009: Geology and Mineral Resources of Nigeria. Lecture note in Earth Sciences, ISSN 9930-0317, Springer Dordrecht Heidelberg, London, New York, 219 p., doi: 10.1007/978-3-540-92685-6.
- Ojo J. S., Olorunfemi M. O., 1995: Geoelectric Mapping of a near Vertical Contact: A Case Study around Erusu, Ikare Area, Southwestern Nigeria. *J. Min. Geol.*, **31**, 2, 151–153.
- Okunubi M. O., Olorunfemi M. O., 2016: Integrated geophysical investigation of remotely sensed suspected fault zones around Iwaraja-Ijebu Ijesa area of Osun State, Nigeria. *Ife J. Sci.*, **18**, 1, 133–145.

- Oladunjoye M. A., Olayinka A. I., Alaba M., Adabanija M. A., 2016: Interpretation of High Resolution Aeromagnetic Data for lineaments study and occurrence of Banded Iron Formation in Ogbomoso Area, Southwestern Nigeria. *J. Afr. Earth Sci.*, **114**, 43–53, doi: 10.1016/j.jafrearsci.2015.10.015.
- Olorunfemi M. O., 2008: Voyage on the skin of the Earth: A geophysical experience. Inaugural Lecture 211. Obafemi Awolowo University, Ile-Ife, Nigeria, 75 p.
- Olorunfemi M. O., 2020: Groundwater exploration, borehole site selection and optimum drill depth in basement complex terrain. Special Publication Series 1. (revised version) (ISSN 0795-6495). Published by the Nigerian Association of Hydrogeologists (NAH), 49 p.
- Olorunfemi M. O., Ojo J. S., Sonuga F. A., Ajayi O., Oladapo M. I., 2000: Geophysical investigation of Karkarku Earth dam embankment. *Glob. J. Pure Appl. Sci.*, **6**, 1, 117–124, doi: 10.4314/gjpas.v6i1.16087.
- Olorunfemi M. O., Olarewaju V. O., Avci M., 1986: Geophysical Investigation of a Fault Zone – Case History from Ile-Ife, Southwestern Nigeria. *Geophys. Prospect.*, **34**, 8, 1277–1284, doi: 10.1111/j.1365-2478.1986.tb00528.x.
- Olorunfemi M. O., Oni A. G., 2019: Integrated geophysical methods and techniques for siting productive boreholes in basement complex terrain of southwestern Nigeria. *Ife J. Sci.*, **21**, 1, 013–25, doi: 10.4314/ijs.v21i1.2.
- Olorunfemi M. O., Oni A. G., Bamidele O. E., Fadare T. K., Aniko O. O., 2020: Combined geophysical investigations of the characteristics of a regional fault zone for groundwater development in a basement complex terrain of South-west Nigeria. *SN Appl. Sci.*, **2**, 1033, doi: 10.1007/s42452-020-2363-6.
- Olorunfemi M. O., Oni A. G., Fadare T. K., Bamidele O. E., 2021: Linear geological structure, traverse orientation and structure resolution and characterisation using 1D and 2D images. *NRIAG J. Astron. Geophys.*, **10**, 1, 170–184, doi: 10.1080/20909977.2021.1902111.
- Oluyide P. O., Nwajide C. S., Oni A. O., 1998: The geology of the Ilorin area. Ministry of Solid Minerals Development, Geological Survey of Nigeria, Bulletin No. 42, 84 p.
- Omenda P., 2018: Geothermal outlook in East Africa: Perspectives for geothermal development. International Geothermal Energy (IGA) presentation.
- Omowumi A., 2018: Electrical resistivity and hydrogeochemical evaluation of septic-tanks effluent migration to groundwater. *Malays. J. Geosci.*, **2**, 2, 1–10, doi: 10.26480/mjg.02.2018.01.10.
- Parasnis D. S., 1986: Principles of Applied Geophysics, 4th ed. London, Chapman and Hall, pp. 33–35.
- Rahaman M. A., 1971: Classification of Rocks in the Nigerian Precambrian Basement Complex. Paper read at Annual Conference of Nigerian Mining, Geological and Metallurgical Society. Dec. 1971. Kaduna, **74**, 17, 4233–4245.
- Rahaman M. A., 1973: The Geology of the Distinct around Iseyin Western State, Nigeria. Ph.D. Thesis, University of Ibadan (unpublished), 268 p.
- Rahaman M. A., 1976: Review of the Basement Complex of Southwestern Nigeria. In: Kogbe C. A. (Ed.): Geology of Nigeria. Elizabeth Publishing Co. Lagos, pp. 41–58.

- Ramesh Babu V., Ram S., Sundararajan N., 2007: Modelling and Inversion of Magnetic and VLF-EM Data with an application to basement fractures: A case study from Raigarh, India. *Geophysics*, **72**, 5, B133–B140, doi: 10.1190/1.2759921.
- Reynolds J. M., 2011: *An Introduction to Applied and Environmental Geophysics*, 2nd ed. John Wiley & Sons, Ltd., 710 p.
- Sangodiji E. E, Olorunfemi M. O., 2013: Geophysical Investigation of a Suspected Foundation Failure at Ogbomoso, Southwestern Nigeria. *Pac. J. Sci. Technol.*, **14**, 2, 522–536.
- Sasaki Y., 1992: Resolution of resistivity tomography inferred from numerical simulation. *Geophys. Prospect.*, **40**, 4, 453–464, doi: 10.1111/j.1365-2478.1992.tb00536.x.
- Sharma P. V., 1987: Magnetic method applied to mineral exploration. *Ore Geol. Rev.*, **2**, 4, 323–357, doi: 10.1016/0169-1368(87)90010-2.
- Sheriff R. E., 1991: *Encyclopedic Dictionary of Exploration Geophysics*, 3rd ed. Society of Exploration Geophysicists (SEG), Tulsa, OK.
- Valtr V., Hanzl P., 2008: Geophysical cross-section through the Bogd fault system in the area of the Chandman rupture, SW Mongolia. *J. Geosci.*, **53**, 2, 193–200, doi: 10.3190/jgeosci.023.